Applied Soft Computing 10 (2010) 296–303

Contents lists available at ScienceDirect

Applied Soft Computing

journal homepage: www.elsevier.com/locate/asoc

A passive auto-focus camera control system

Chih-Yung Chen [a,*], Rey-Chue Hwang [b], Yu-Ju Chen [c]

[a] Department of Computer and Communication, Shu-Te University, Kaohsiung County 840, Taiwan
[b] Department of Electrical Engineering, I-Shou University, Kaohsiung County 840, Taiwan
[c] Information Management Department, Cheng-Shiu University, Kaohsiung County 833, Taiwan

ARTICLE INFO

Article history:
Received 3 July 2007
Received in revised form 12 July 2009
Accepted 26 July 2009
Available online 4 August 2009

Keywords:
Passive
Auto-focus system
Sharpness measurement
Discrete wavelet transformation
Self-organizing map
Morphology

ABSTRACT

This paper presents a passive auto-focus camera control system which can easily achieve the function of auto-focus with no necessary of any active component (e.g., infrared or ultrasonic sensor) in comparison with the conventional active focus system. To implement the technique we developed, the hardware system including the adjustable lens with CMOS sensor and servo motor, an 8051 image capture micro-controller, a field programmable gate array (FPGA) sharpness measurement circuit, a pulse width modulation (PWM) controller, and a personal digital assistant (PDA) image displayer was constructed. The discrete wavelet transformation (DWT), the morphology edge enhancement sharpness measurement algorithms, and the self-organizing map (SOM) neural network were used in developing the control mechanism of the system. Compared with other passive auto-focus methods, the method we proposed has the advantages of lower computational complexity and easier hardware implementation.

1. Introduction

With the rapid development of digital still camera (DSC) technology, auto-focus has become an important function and widely used in many mobile devices such as cellular phone, notebook, and personal digital assistance (PDA). The picture taken by a camera without auto-focus function could be incorrect and blurred. Generally, the high-level DSC must have the active focus component such as infrared or ultrasonic sensor which can measure the distance between camera and object. The camera lens then can be adjusted and move to an appropriate position to clearly focus the object desired. It is a well-known technique commonly used by DSC manufacturer. Undoubtedly, such an active focus component design in DSC will have some drawbacks such as the increasing of product's cost and more battery power.

It is well-known that an alternative way to achieve the focus function of camera is the passive auto-focus technique. Basically, the photo's definition plays an important role for a captured image. Therefore, the performance of sharpness measurement algorithm will mainly determine the efficiency of passive auto-focus component's function. Currently, the presented sharpness measurement approaches can be divided into two categories, i.e., the spatial and frequency domain measurements. The spatial method, Laplacian, Sobel gradient [1], and statistical approachs [2,3] can determine the sharpness with respect to the edge information or gradient magnitude of image. The frequency methods, such as the fast Fourier transform (FFT) [4], discrete cosine transform (DCT) [5], and discrete wavelet transform (DWT) [6], can determine the sharpness by using the high-frequency components of image. In general, the performance by frequency domain based measurement is better than the spatial way due to its better capability in anti-noise. However, the frequency domain based measurement usually has the problem of higher computational complexity.

In this study, a passive auto-focus control system with lower complex computation on frequency measurement was developed. This control system not only can make DSC cost be reduced, but also can be designed as an application-specific integrated circuit (ASIC). In the proposed scheme, both Lifting 5/3 DWT and edge enhancement algorithm were used to measure the sharpness which is the judge criterion to indicate whether the system is on accurate focus or not. The servo motor and self-organizing map (SOM) neural network based controller were employed to make camera's lens reach to the accurate position. Furthermore, the field programmable gate array (FPGA) implementation and practical platform were taken to demonstrate the focus performance of this scheme which could be potentially used to design a high-performance DSC with the passive auto-focus function.

2. Auto-focus system

Most of high-level DSCs provide focusable function which can improve the quality of image. Basically, the theorem of object

* Corresponding author.
E-mail addresses: mikechen@mail.stu.edu.tw (C.-Y. Chen), rchwang@isu.edu.tw (R.-C. Hwang), yjchen@csu.edu.tw (Y.-J. Chen).

1568-4946/$ – see front matter © 2009 Elsevier B.V. All rights reserved.
doi:10.1016/j.asoc.2009.07.007

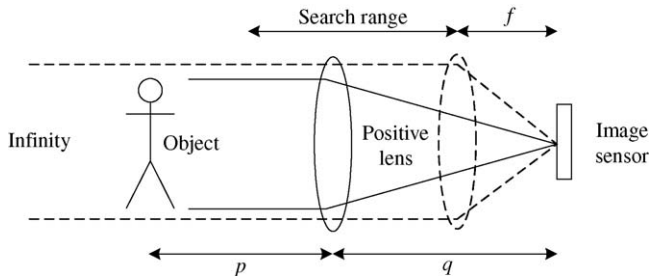

Fig. 1. The diagram of camera focus.

captured by camera and the formation of image are shown in Fig. 1. All parallel rays are focused to a point which is referred to as the principal focal point, i.e., the position of image sensor. The distance from lens to this point is given by the principal focal length f which is set by the lens manufacturer according to the parameters of lens. Let the distance between camera's lens and a captured object be p, the distance between lens and the principle focal point be q, then the relationship among distances f, p and q can be expressed by Eq. (1).

$$\frac{1}{f} = \frac{1}{p} + \frac{1}{q} \tag{1}$$

2.1. Active auto-focus system

In the process of photo shooting, the correct lens position could be manually adjusted based on user's experience. In the active auto-focus system, active component such as infrared rays or ultrasonic component is used to help the lens to reach a suitable position. Basically, the distance p between DSC and object can be estimated by these active components. Once the value of p is obtained, the proper value of q for lens position can be automatically controlled by an established motor controller in order to fit Eq. (1). However, as mentioned above, additional active component will certainly increase the cost, size, and power consumption of the camera system. They are obviously the disadvantages for designing a slimmer, low-cost and low-power mobile device.

2.2. Passive auto-focus system

Passive auto-focus (PAF) is a technique to find the best focused lens position without active component [7]. One of PAF methods is to use the image processing algorithm to estimate the sharpness of picture. A good sharpness measurement algorithm should obtain the higher sharpness value for the proper lens position to a well-focused image than an improper one. The curve C (a similar Gaussian curve) of sharpness values versus lens position is shown in Fig. 2. In this figure, the highest sharpness value can be obtained when the lens is on the well-focused position s_w. However, the best focused lens position is hard to find by using conventional PAF algorithm. Thus, the full search is usually required.

Basically, the proposed passive auto-focus system is based on machine vision if no any active component is used. In our study, DWT and morphology edge enhancement algorithm were used for the sharpness measurement. Furthermore, SOM neural network controller was designed to control the adjustable lens to reach an accurate position. Fig. 3 shows the flowchart of the proposed scheme we developed. All methods used in this system emphasize that the sharpness could be measured correctly and easily to be implemented as hardware or embedded system. The details of each function block are described in the following sections.

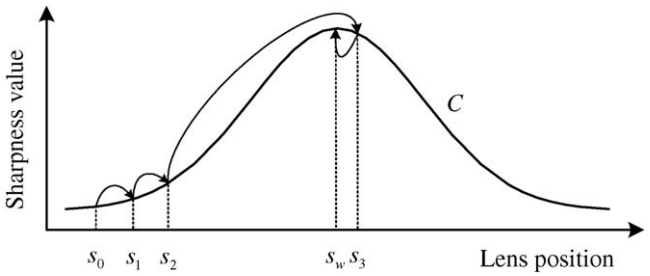

Fig. 2. The passive focus sharpness curve.

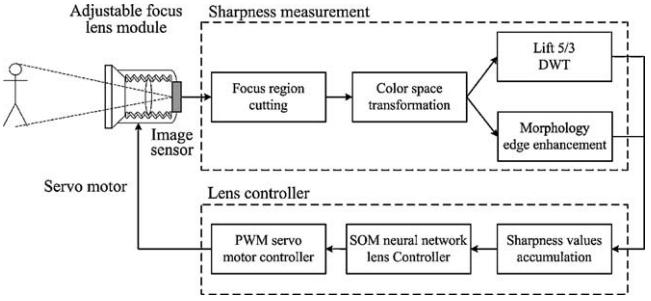

Fig. 3. The flowchart of the proposed system.

3. The algorithms for sharpness measurement

In general, the high-frequency signal and edge information of an image are the sharpness basis for human's vision system. The high-pass filter of image processing is usually taken as the sharpness measurement component. DWT computation can separate the signals on high-frequency band from original image and these signals then can be used to do the sharpness value's estimation. In addition, the morphology edge enhancement algorithm is a high-performance and low-complexity edge detector. In this study, both methods were simultaneously employed into the measurement of image sharpness.

3.1. DWT sharpness measurement

DWT method has been proved its validity in sharpness measuring. The detailed mathematical model is shown in articles [8,9]. In DWT, Lifting 5/3 [10] is the simplest one which is shown in Fig. 4. Due to the characters of low complexity and easy hardware implementation, it was selected and used in developing the system proposed. The procedure of Lifting 5/3 DWT can be mainly divided into two steps:

1. *Splitting step*: In this step, a raw data R with length n can be divided into two parts, the odd points r_{2i+1} and even points r_{2i}. They are denoted as S_i^0 and D_i^0, respectively. Their mathematical expressions are given by
$$S_i^0 = r_{2i+1}, \quad D_i^0 = r_{2i}, \quad \forall (r_{2i+1}, r_{2i}) \in R, \quad \text{and} \quad i = 0, 1, 2, \ldots, \frac{n}{2} \tag{2}$$
2. *Lifting step*: The high-pass elements D_i^1 and low-pass elements S_i^1 can be calculated by
$$D_i^1 = D_i^0 - \frac{(S_i^0 + S_{i+1}^0)}{2} \tag{3}$$
$$S_i^1 = S_i^0 + \frac{(D_{i-1}^1 + D_i^1)}{4} \tag{4}$$

In image processing, the captured two-dimensional image can be firstly transformed by using both horizontal and vertical

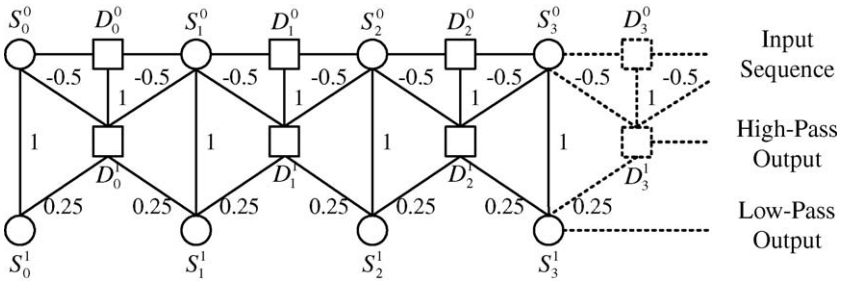

Fig. 4. Lift 5/3 DWT diagram.

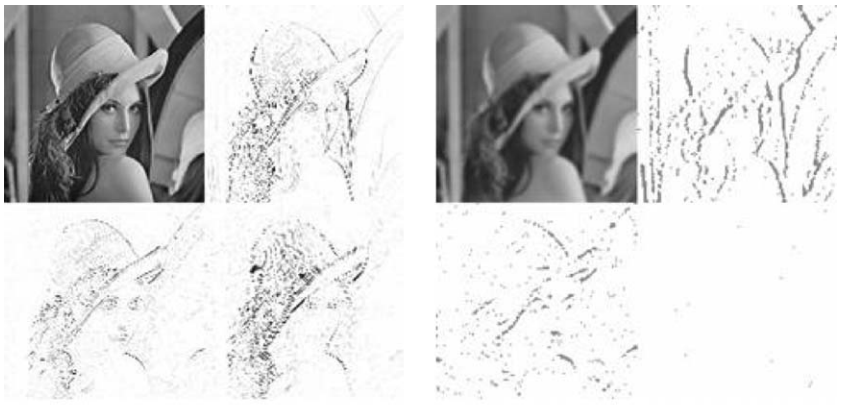

Fig. 5. Frequency bands of DWT. (a) The focused image and (b) the blurred image.

Lifting transformations. The image then can be divided into four bands, i.e., {*LL*, *LH*, *HL*, *HH*}, where *L* and *H* stand the low-band and the high-band, respectively. Due to the sharpness only regards to the high-band signals, therefore the signals on *HH* band (i.e., the right-bottom quarter of the image) are taken to evaluate the sharpness of image. For a captured image $\mathbf{X}$ and its DWT transformed image $\tilde{\mathbf{X}}$ with n rows and m columns, the sharpness measurement function $h(\cdot)$ can be calculated by

$$\forall \tilde{x}_{i,j} \in \tilde{\mathbf{X}} \quad \text{and} \quad h(\tilde{\mathbf{X}}) = \sum_{i=n/2}^{n} \sum_{j=m/2}^{m} \tilde{x}_{i,j} \tag{5}$$

where i and j are the row and column indexes of image $\tilde{\mathbf{X}}$.

In the proposed system, Lifting 5/3 DWT was implemented by FPGA. Fig. 5 shows the transformed results by using Lifting 5/3 DWT hardware to a focused image and a blurred image. Obviously, the amount of signals on the high-frequency band of the focused image is much more than the blurred image.

3.2. Morphology sharpness measurement

The idea of mathematical morphology was initialized by Matheron [11]. Subsequently, Serra proposed the theory which includes set theory, geometry and algebra in year 1982 [12]. The morphology image processing can be applied to the enhancement of image, the image restoration and the edge detection, etc. In the application of machine vision, the edge image has been widely studied. The edge image not only can clearly describe the sketch of a picture's boundary, but also can efficiently estimate the sharpness of image. The morphology edge enhancement is generally employed into the sharpness measurement due to its computationally efficient. However, only grey-scale operations are discussed in this study.

In the morphology image processing, dilation, erosion, opening, and closing are four basic operators. For a briefly explanation, only dilation is reported in this paper. Moreover, the morphology image processing mainly operates the structuring element which is a set of neighborhood pixels. The proper structuring element assignment could improve the processing result. For describing the morphology implementation, suppose there is an image $\mathbf{X}$ with n rows and m columns, in which each pixel is denoted as $x_{i,j}$. A two-dimensional structuring element U with size $n_s \times n_s$ is defined. The operations are described as follows:

1. *Dilation*: In image processing, dilation operation can extend the boundary of an object by removing the low valued regions. After the dilation operation, new pixel $x'_{i,j}$ can be obtained by the following equation:
$$x'_{i,j} = x_{i,j} \oplus U = \max\{x_{i+(a-n/2),j+(b-n/2)} + u_{a,b}\} \tag{6}$$
where $u_{a,b} \in U$ and $0 \le a, b \le n_s$.
2. *Edge enhancement*: The edge detector of image segmentation usually has a huge computational complexity. However, the morphology edge enhancement listed in Eq. (7) is simple and efficient. The operation of each pixel includes one subtraction and one dilation.
$$\hat{x}_{i,j} = (x_{i,j} \oplus U) - x_{i,j} \tag{7}$$

Fig. 6 shows the edge enhancement results of the well-focused and blurred images, respectively. Obviously, compare with the blurred image, the higher edge enhancement effect can be found in the well-focused image. Thus, all obtained $\hat{x}_{i,j}$ pixels (i.e., the preformed image $\hat{\mathbf{X}}$) can be summed up for the sharpness measurement and expressed as

$$p(\hat{\mathbf{X}}) = \sum_{i=1}^{n} \sum_{j=1}^{m} \hat{x}_{i,j} \tag{8}$$

where i and j are the row and column indexes of image $\hat{\mathbf{X}}$.

Fig. 6. The edge enhancement results of the well-focused and blurred images. (a) The focused image and (b) the blurred image.

3.3. The proposed hybrid sharpness measurement

As mentioned previously, both Lift 5/3 DWT and morphology edge enhancement are feasible for the sharpness measurement. However, these two methods are still not very stable while they are used independently under a variable environment. In our study, both methods are combined to be a hybrid tool which is more reliable and stable in the sharpness measurement.

It is known that it will take much time for a sensor in capturing an entire image. Therefore, during the focusing procedure, only the focus region in a captured image is taken for the sharpness measurement. The focus region **R** of a captured image **X** can be expressed as

$$\mathbf{R} = \{x_{i,j} | \forall x_{i,j} \in \mathbf{X}, \alpha_1 < i < \alpha_2, \beta_1 < j < \beta_2\} \tag{9}$$

where α_1, β_1 and α_2, β_2 are the boundary coordinates of the focus region.

Basically, the colour image captured by CMOS sensor consists of red, green and blue channels. In human's vision system, the luminance is an important factor for sharpness measurement. Hence, a *RGB* to YCrCb colour space transformation is taken to obtain luminance component *Y* before the sharpness measurement. The transformation is generally given by

$$\begin{bmatrix} Y \\ Cr \\ Cb \end{bmatrix} = \begin{bmatrix} 0.299 & 0.587 & 0.114 \\ -0.169 & -0.331 & 0.5 \\ 0.5 & -0.419 & -0.081 \end{bmatrix} \times \begin{bmatrix} R \\ G \\ B \end{bmatrix} \tag{10}$$

Due to the floating point computation is not efficient to design as hardware; the modified *Y* transformation is redefined by the following equation according to the characteristic of COMS sensor.

$$Y = \lfloor \frac{R}{4} + \frac{G}{2} + \frac{B}{4} \rfloor + \frac{1}{8} \lfloor \frac{R}{4} + \frac{G}{2} + \frac{B}{4} \rfloor \tag{11}$$

In the hardware design, the denominators 2, 4 and 8 are shifted by shifting registers for 1, 2 and 3 bits, respectively. In our experiments, the result of Eq. (11) could achieve the same goal as Eq. (10) but no multiplier circuit is needed. After transformation, the transformed *Y* component image can be the grey-scale input image of the sharpness measurement. Then, the proposed sharpness measurement function $M(\cdot)$ which combines two sharpness functions $h(\cdot)$ and $p(\cdot)$ shown in Eqs. (5) and (8) can be given by

$$M(\mathbf{R}) = k_1 h(\bar{\mathbf{R}}) + k_2 p(\hat{\mathbf{R}}) \tag{12}$$

where k_1 and k_2 are constants, $\bar{\mathbf{R}}$ and $\hat{\mathbf{R}}$ are DWT and edge enhancement performed images, respectively.

In our experiments, k_1 and k_2 are set as 0.6 and 0.4, respectively. The ideal curve of sharpness versus lens position could be generally described as Gaussian curve. Fig. 7 shows the comparison between the ideal and practical results calculated by the proposed approach with different focused images. The diagram clearly illustrates the feasibility of the sharpness measurement we adopted.

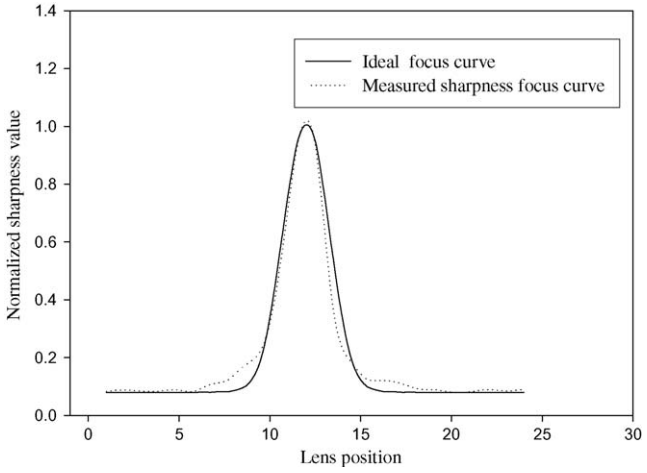

Fig. 7. The comparison of sharpness curves versus lens positions.

4. SOM neural network controller

In the active auto-focus system, the best focused lens position is determined by the distance between object and camera. In PAF system, the best focused lens position searching needs to consider the optimal focused sharpness value. But, the optimal focused sharpness value of a scene is usually unknown before the best focused position is reached. Such an optimal sharpness must be searched step by step; it is so-called the mountain climbing problem [13]. In this study, a SOM neural network based controller is designed to find the best focused lens position. The detailed proposed scheme is stated completely in this section.

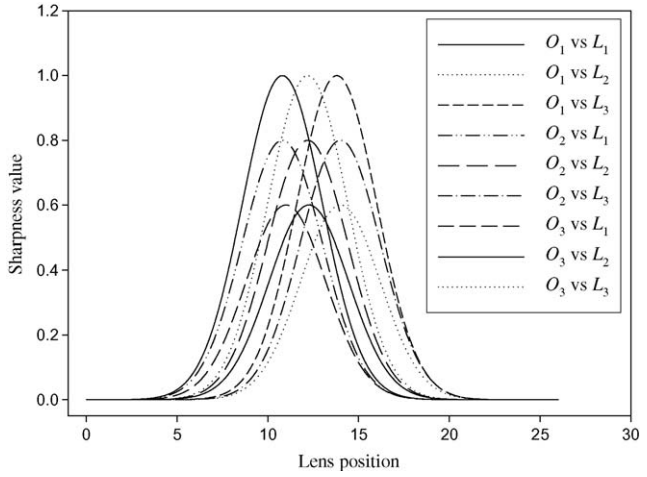

Fig. 8. Sharpness values of different objects with different lens positions.

4.1. Best focused lens position searching problem

To explain the best focused lens position searching problem we proposed, the sharpness values of three objects O_1, O_2 and O_3 with different distances L_1, L_2 and L_3 between the object and camera are discussed. Fig. 8 shows the curves of each sharpness value versus lens positions; all values were calculated by the proposed sharpness measurement algorithm. From the figure shown, the sharpness values of a captured image are various for different objects (i.e., scenes). The best focused value is always unknown in each focus process. Thus, full search is usually needed for a clear image capturing. Undoubtedly, such a searching way is not efficient due to the time wasting in many lens movements.

As mentioned above, the best focused lens position is not easily to be obtained. A best position searching must involve two requirements, i.e. the time saving of the image capturing and the fast moving of lens to an appropriate position without additional steps. In our study, a SOM neural network controller was designed to achieve such a goal.

4.2. SOM neural network

Self-organizing map (SOM) neural network is a well-known unsupervised learning neural model that was introduced by Kohonen [14]. The training process of SOM neural network is based on competitive learning algorithm. Fig. 9 shows a two-dimensional SOM neural network structure.

The input layer and Kohonen layer are defined as vectors $\mathbf{s}$ and $\mathbf{k}$ respectively, and given by

$$\mathbf{s} = [s_1, s_2 \ldots, s_n]^T \quad \text{and} \quad \mathbf{k} = \begin{Bmatrix} k_{11} & \cdots & k_{1b} \\ \vdots & \ddots & \vdots \\ k_{a1} & \cdots & k_{ab} \end{Bmatrix} \tag{13}$$

where n is the length of input layer (i.e. test data), a and b are the lengths of row and column of Kohonen layer.

Each neuron k in Kohonen layer $\mathbf{k}$ has the same dimension as input space $\mathbf{s}$. Thus, a weight vector $\mathbf{w}_i$ of k can be expressed as

$$\mathbf{w}_i = [w_{i1}, w_{i2}, \ldots, w_{in}]^T \quad \text{and} \quad \forall_{i \in I} k_i \in \mathbf{k} \tag{14}$$

where I is the index number of Kohonen layer $\mathbf{k}$.

The input vector $\mathbf{s}$ is fully connected to the array of Kohonen layer $\mathbf{k}$ by the weight vector $\mathbf{w}_i$. $\mathbf{k}$ is the training data which is the representative sharpness values of the fixed lens positions s_0, s_1, and s_2. Additionally, the training data includes the complex or bright image with high sharpness value, and the plain or dark image with low sharpness value. All representative images were taken by different lens positions. In this case, 9 categories in the output layer need to be classified, e.g., k_{11} is the category of O_1 with distance L_1 and k_{33} is the category of O_3 with distance L_3. Moreover, the initial values of weight vector $\mathbf{w}_i$ could be determined randomly.

The best-matching neuron of the input vector can be found by minimizing the Euclidean distance between $\mathbf{s}$ and $\mathbf{w}_i$ two vectors. Suppose the best-matching neuron index (i.e., the winner's index) of the input layer $\mathbf{s}$ is denoted as $b(\mathbf{s})$, then it can be determined by the following condition:

$$b(\mathbf{s}) = \arg\min_i \|\mathbf{s} - \mathbf{w}_i\| \tag{15}$$

Once the best-matching neuron was found, the weight vectors then can be updated. The formula of weight vector adjustment is expressed as

$$\mathbf{w}_i(t+1) = \mathbf{w}_i(t) + \eta(t) h_{i,b(s)}(t)(s - \mathbf{w}_i(t)) \tag{16}$$

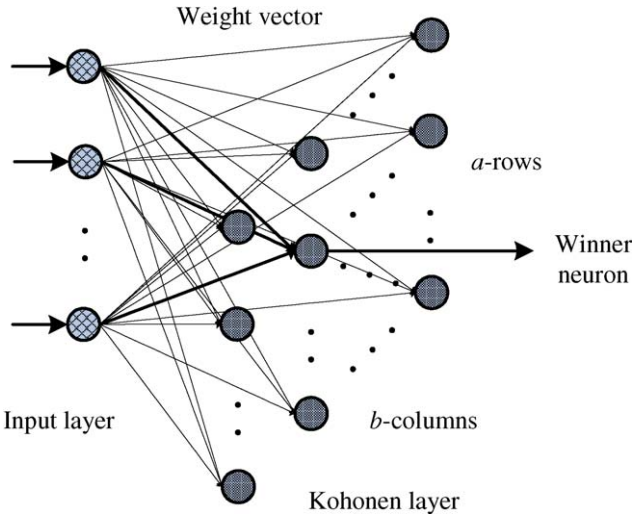

Fig. 9. SOM neural network model.

where t is discrete time index, $\eta(t)$ is the learning rate, and $h_{i,b(\mathbf{s})}(t)$ is the neighborhood function centered around the winning neuron $b(\mathbf{s})$.

In the system we proposed, the neural network is firstly trained by an offline process. The well-trained SOM neural network is used to predict the best focused lens position. Once the input data is measured, the trained SOM neural network can determine the output category. Then, the controller can move lens to the pre-defined best focused position in accordance with the category determined. In other words, the accuracy of neural network plays a critical role in the whole control process. The pre-defined focused position (i.e. the revolutions of servo motor) can be given by $\mathbf{z}$ as shown in Eq. (17) which has the same dimensions as $\mathbf{k}$. In the hardware design, it can be stored in the read-only memory.

$$\mathbf{z} = \begin{Bmatrix} z_{11} & \cdots & z_{1b} \\ \vdots & \ddots & \vdots \\ z_{a1} & \cdots & z_{ab} \end{Bmatrix} \tag{17}$$

4.3. Proposed SOM neural network searching method

As mentioned above, a well-trained SOM neural network is used to find the best lens position and to avoid the time waste. Here, a new search method with prediction technique is proposed to explain how to determine the best lens position. As shown in Fig. 10, the lens returns to its start position at the beginning of PAF procedure. Three samples are measured firstly to predict the best focused position by using the well-trained neural model. As shown in Fig. 2, the sharpness values of three lens positions s_0, s_1 and s_2 (i.e. the input data of SOM neural network) are used to predict the candidate of the best focused position s_3 (i.e. the desired output). The lens will move to s_3 and then go back to search the maximum focused value more exactly. Thus, the best focused position s_w is easily to be obtained by a backward search.

5. Embedded system and hardware implementation

In our study, a PAF platform was built as shown in Fig. 11 to implement the control techniques we proposed. It consists of an adjustable lens module, a microprocessor, a FPGA chip and a PDA displayer. The detailed functionality of each block is described as follows.

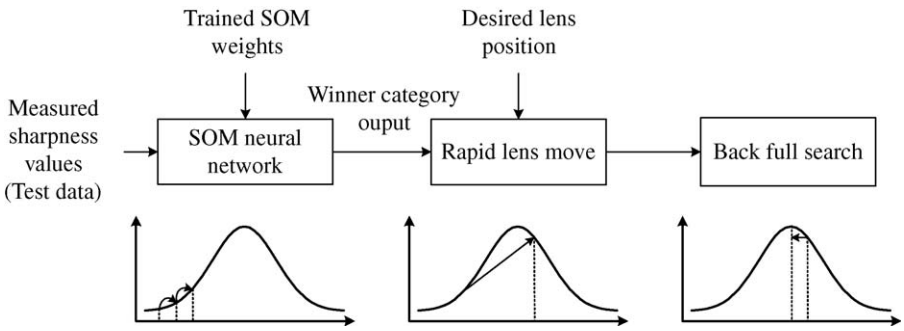

Fig. 10. The proposed searching method.

5.1. Adjustable lens module

To build the prototype of proposed platform, a CMOS type image sensor with 100 K color pixels (i.e., 352 × 288) was used to capture images. Subsequently, an adjustable lens connected with a continuous rotation servomotor was applied to control the lens position. The servomotor is controlled by the pulse width modulation (PWM) signal. The frame time of PWM is approximately 20 ms. The positive pulse is normally within 0.9 ms and 2.1 ms. To the continuous rotation servomotor, 0.9 ms, 1.5 ms and 2.1 ms positive pulses can make it rapidly forward rotate, hold steadily and rapidly backward rotate, respectively. Moreover, for instance, if a servomotor received a 1.6 ms pulse with 20 ms then it will rotate forward slowly. Thus, the lens can be controlled to move forward or backward, fast or slow. The appearance of this module is shown in Fig. 12.

5.2. FPGA hardware design

In the system developed, all algorithms used were focused on easy implementation by the hardware. Lift 5/3 DWT, morphology edge enhancement, and PWM controller are all implemented by a FPGA chip (*Altera* Cyclone EP1C12Q240C8). The related hardware design methodologies can be found in the articles [15,16].

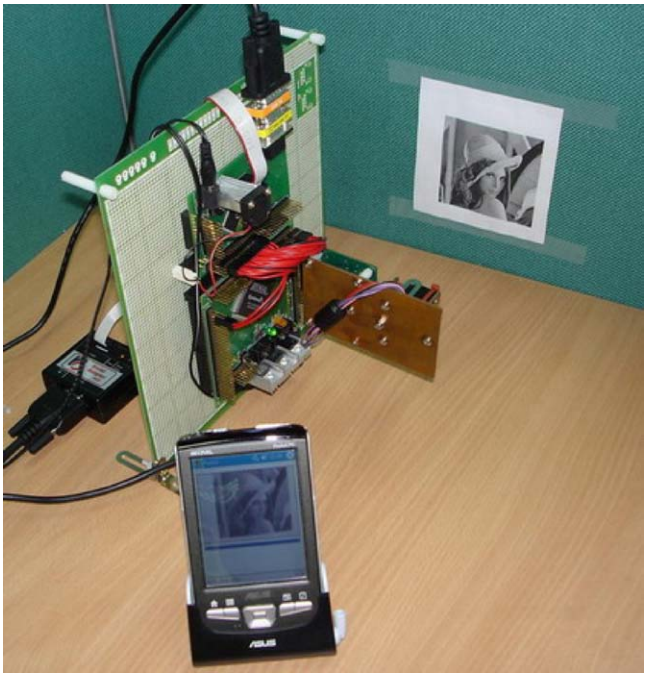

Fig. 11. The proposed PAF platform.

5.3. Microprocessor

Except FPGA, a microprocessor was applied to be the controller for communications among the designed modules. The system clock of high-speed 8051 microprocessor used is 100 MHz and the size of external SRAM is 64 KB. The microprocessor provides several functions including image capturing, FPGA components communication and lens controller implementation (i.e., SOM neural network).

5.4. PDA displayer

A PDA was used as the human interface device which was designed by using the embedded graphical software developer *Microsoft* .NET Framework. The software is operated under the Windows Mobile 2003 operation system. Therefore, the lens position can be controlled and the captured image can be displayed by this PDA displayer. This also shows the validity of proposed approach which could be designed suitably as an embedded system.

6. Experimental results

To evaluate the performance of proposed system, this section presents the results of the sharpness measurement approach and search algorithm. Besides, the simulation results of each hardware function block implemented by *Altera* Quartus II 5.0 are shown in Table 1.

6.1. Sharpness measurement results

In the simulations of sharpness measurement, the test images including Lena, Baboon and Peppers, etc., were blurred by Gaussian function with different standard deviation σ from 0.3 to 3. Fig. 13

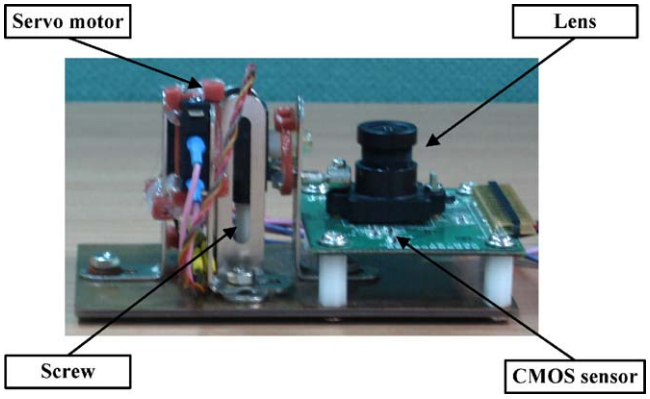

Fig. 12. Adjustable lens module.

Table 1
The performances of FPGA function blocks.

	Logic elements	Most critical path delay	Performance
Pulse width modulation	56	3.006 ns	190 MHz
Lift 5/3 DWT	346	4.895 ns	179 MHz
Morphology edge enhancement	334	6.878 ns	128 MHz

Table 2
The comparison of best focused position search.

Methods	Steps			
	Average	Maximum	Minimum	Standard deviation
The proposed algorithm	7.2	12	5	1.76
Full search	18.3	21	16	1.58

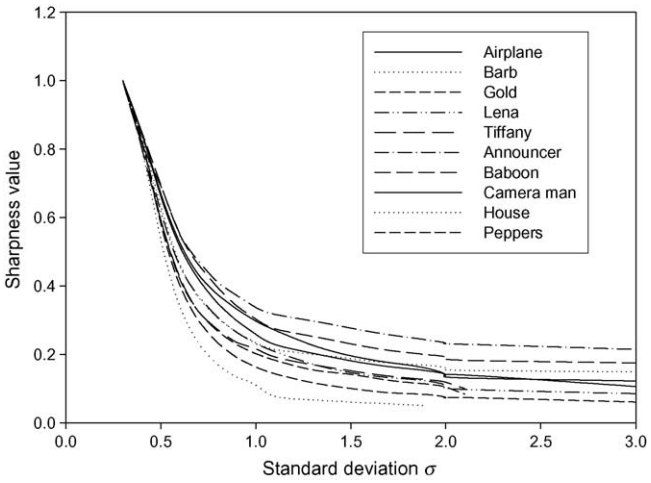

Fig. 13. The results of proposed sharpness measurement approach.

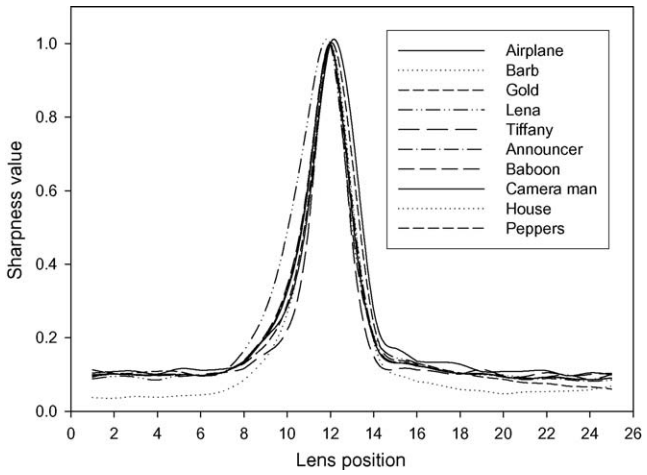

Fig. 14. The results of the sharpness measurement for different lens positions.

shows the measured results of proposed sharpness measurement approach.

In the practical experiment, the original test images were printed and used as the capturing target by the platform proposed. Fig. 14 illustrates the results of measured sharpness by using the sharpness measurement hardware at different lens positions. Clearly, all captured test images display the similar Gaussian curves. That means the proposed sharpness approach performs quite well by the lens and image sensors we used.

6.2. Best focused lens position searching results

In our previous discussion, SOM neural network was used for the best focused lens position searching and it was trained offline firstly. In our study, the size of SOM is set as 5×5 SOM (i.e., 25 categories) due to the limit of ROM size of microprocessor. For determining the best parameters and training result of neural network, different learning rates within the range from 0.8 to 1.0 were tested. At each trial, the increment of learning rate is 0.001. In addition, at each training process for the specific learning rate, the neural model was executed from 50 to 300 iterations with an increase of 10 each time in order to find the best training iteration. Finally, we concluded that the best parameters of SOM can be obtained at the learning rate 0.977 and at the iteration number 100. Once the training process is finished, the weights then can be stored in the microprocessor's ROM (300 bytes). This well-trained SOM neural network can be implemented as firmware in the microprocessor. The classification procedure takes about 600

Fig. 15. The images of focus procedure.

clocks (i.e., operations) to classify the category of three input samples. Basically, microprocessor will take much time in the image capturing and the sharpness measuring for a conventional PAF. In Table 2, the comparison of the proposed search method and full search method is reported. In this table, the step stands the time of lens moving and image capturing. Clearly, the proposed search method only takes 7.2 steps averagely for 50 test cases. Fig. 15 shows the results of focus process of the proposed method. The image was immediately focused in six steps. Compare with the full search method, we clearly find that the approach proposed can greatly reduce the search time for an accurate focused lens position searching.

7. Conclusions

In this paper, a passive auto-focus control system was designed and the new sharpness measurement scheme with SOM neural network based searching strategy was also proposed. Easy implementation by hardware, no active component, rapid auto-focus and low image processing complexity are the advantages of the system we developed. Nowadays, the well function of camera is required by most of mobile devices such as PDA, DSC, and mobile phone. Most of high-end camera embedded devices have auto-focus system to capture high-quality image. However, due to the mobile device has no extra power and space to contain the active focus component, the proposed PAF scheme indeed has the great potential to achieve such a goal in the real applications. Furthermore, the proposed SOM neural network could predict the accurate focus lens position. It is an innovation to the current auto-focusing system. The searching performance could be greatly improved in comparison with the full searching strategy commonly used.

In our study, the experimental results have shown the superiority of the sharpness measurement scheme we proposed. However, in real case, the accurate estimation of the sharpness for an image with lower or excessive illumination is not easy. The inaccurate sharpness measurement will directly affect the best focus lens position searching. Thus, in our future works, a more powerful and accurate sharpness measurement algorithm which is more suitable for various environments is still worthy of our continued study.

References

[1] E.P. Krotkov, Active Computer Vision by Cooperative Focus and Stereo, Springer-Verlag, New York, 1989.
[2] Y.N. Zhang, Y. Zhang, C.Y. Wen, A new focus measure method using moments, Image Vis. Comput. 18 (12) (2000) 959–965.
[3] C.Y. Wee, P. Raveendran, Measure of image sharpness using eigenvalues, Inf. Sci. 177 (12) (2007) 2533–2552.
[4] E.R. Davies, Machine Vision: Theory, Algorithms Practicalities, Academic Press, 1990.
[5] J. Baina, J. Dublet, Automatic focus and iris control for video cameras, in: Fifth International Conference on Image Processing and its Applications, Edinburgh, UK, 1995, pp. 232–235.
[6] S.Y. Lee, Y. Kumar, J.M. Cho, S.W. Lee, S.W. Kim, Enhanced autofocus algorithm using robust focus measure and fuzzy reasoning, IEEE Trans. Circuits Syst. Video Technnol. 18 (9) (2008) 1237–1246.
[7] M. Subbarao, J.K. Tyan, The optimal focus measure for passive auto focusing and depth from focus, in: Proceedins of SPIE Conference on Videometrics IV, Philadelphia, (1995), pp. 89–99.
[8] J. Kautsky, J. Flusser, B. Zitova, S. Simberova, A new wavelet-based measure of image focus, J. Pattern Recogn. Lett. 23 (14) (2002) 1785–1794.
[9] J.T. Huang, C.H. Shen, S.M. Phoong, H.H. Chen, Robust measure of image focus in the wavelet domain, in: International Symposium on Intelligent Signal Processing and Communication Systems, Hong Kong, (2005), pp. 157–160.
[10] I. Daubechies, W. Sweldens, Factoring wavelet transforms into lifting schemes, J. Fourier Anal. Appl. 4 (1998) 247–269.
[11] G. Matheron, Random Sets and Integral Geometry, John Wiley and Sons, New York, 1975.
[12] J. Serra, Image Analysis and Mathematical Morphology, Academic Press, London, 1982.
[13] J. He, R. Zhou, Z. Hong, Modified fast climbing search autofocus algorithm with adaptive step size searching technique for digital camera, IEEE Trans. Consumer Electron. 49 (2) (2003) 257–262.
[14] T. Kohonen, Self-Organizing Maps, Springer-Verlag, Berlin, 1995.
[15] H. Liao, M.K. Mandal, B.F. Cockburn, Efficient architectures for 1-D and 2-D lifting-based wavelet transforms, IEEE Trans. Signal Process. 52 (5) (2004) 1315–1326.
[16] H. Hedberg, F. Kristensen, V. Owall, Low-complexity binary morphology architectures with flat rectangular structuring elements, IEEE Trans. Circuits Syst. 55 (8) (2008) 2216–2225.